Fluoride 2019 June 9. www.fluorideresearch.online/epub/files/042.pdf [Epub ahead of print]

MODELING AND OPTIMIZATION OF FLUORIDE ADSORPTION FROM AQUEOUS SAMPLES BY AMMONIUM ALUMINIUM SULFATE USING RESPONSE SURFACE METHODOLOGY (RSM)

Mojtaba Afsharnia,[a] Mahmood Shams,[b] Mehdi Ghasemi,[a,] Hamed Biglar,[a]
Samira Salari,[a,]* Asiyeh Moteallemi[c]
Gonabad, Mashhad, and Torbat Jam, Iran

ABSTRACT: The aim of the present study was to study the removal of fluoride from synthetic aqueous solutorganicions by ammonium aluminium sulfate $(NH_4)Al(SO_4)_2$. Response surface methodology (RSM) was employed in order to optimize and analyse the operating variables of the initial fluoride concentration, the sorbent dosage, the pH, and the contact time. The maximum percentage removal of fluoride in the optimum conditions (initial fluoride concentration = 6.80 mg/L, adsorbent dose = 3.25 g/L, pH = 9, and time = 16.5 min) was 100%. The high value of the coefficient of determination (R^2=0.97) indicated the adequacy of the linear model to predict the removal of fluoride. Isotherms results showed that the Freundlich model provided the best fit for the fluoride adsorption. The experimental data also followed closely the pseudo second-order kinetic model with a correlation coefficient of 0.99. This study revealed that ammonium aluminium sulfate is an efficient adsorbent for the removal of fluoride.

Key words: Adsorption, Modeling, Ammonium aluminium sulfate

INTRODUCTION

Fluoride, particularly as a topical application, is used in several countries to prevent and treat dental caries.[1] However, the continuous consumption of drinking water containing excessive amounts of fluoride can result in various problems such as dental and skeletal fluorosis, and the various forms of non-skeletal fluorosis including thyroid disorder, brain damage, renal and hepatic impairment, and osteosarcoma.[2-7] Many studies have shown a fluoride level in water sources, particularly ground water, that is higher than the upper acceptable level recommended by the WHO (1.5 mg/L) in the many parts of world, including Africa, Mexico, India, and China.[8-10] Also in some of regions in Iran, the fluoride concentration is above the guideline value of WHO. [11-13] High levels of fluoride in drinking water can occur from either geological deposits or industrial wastewater contaminated with fluoride such as from glass and ceramic manufacturing industries,[14] aluminum and zinc smelters,[15] and superphosphate fertilizer and semiconductors production industries.[16,17] During recent decades, in order to remove fluoride from drinking water, various techniques have been used such as ion exchange,[18] precipitation,[19] reverse osmosis,[20] electrodialysis,[21] Donnan dialysis,[22] nanofiltration,[23] and adsorption.[24,25] Among these techniques, the adsorption process is a cost effective method with a simple method of operation for the removal of excessive fluoride from drinking water. Considering this issue, many adsorbents have been developed such as modified activated carbons,[26] chitin, chitosan,[27] zeolite,[28] and modified ferric hydroxide.[29] Ammonium aluminum sulfate (ammonium alum) is

---

[a]Department of Environmental Health Engineering, School of Public Health, Gonabad University of Medical Sciences, Gonabad, Iran; [b]Department of Environmental Health Engineering, School of Public Health, Mashhad University of Medical Sciences, Mashhad, Iran; [c]Department of Environmental Health Engineering, School of Nursing, Torbat Jam Faculty of Medical Sciences, Torbat Jam, Iran. *For correspondence: Samira Salari, Department of Environmental Health Engineering, School of Public Health, Gonabad University of Medical Sciences, Gonabad, Iran; E-mail: samirasalari481@yahoo.com

a white crystalline double sulfate that can be applied in water treatment due to its inexpensive, nontoxic and availability properties.[30]

The application of the conventional method of studying a process, by changing only one factor at a time while keeping the other factors constant, cannot determine the interactive effects of all the factors involved. In addition, this method requires a large number of experiments for the determination of the optimum conditions and is time-consuming. The limitations of the conventional method can be reduced by statistical experimental design such as by using response surface methodology (RSM). RSM is a collection of statistical techniques whose main goal is optimizing processes and the evaluation of the main and the interactive effects of factors.[31] The main objectives of the present study were the modeling and optimization of fluoride adsorption from synthetic aqueous solutions by ammonium aluminum sulfate $(NH_4)Al(SO_4)_2$ (AAS) using response surface methodology (RSM). Also, the influence of co-existing anions, the adsorption kinetics, and the adsorption isotherm were investigated.

MATERIALS AND METHODS

Preparation of ammonium aluminum sulfate (AAS): Ammonium aluminum sulfate (AAS) was placed in a furnace at 350ºC for 30 minutes and then cooled in a desiccator. Finally, it was crushed in a mortar and sieved through 10 and 30 mesh screens to obtain uniform particles and used for the experiments. Figure 1 shows ammonium aluminum sulfate before and after thermal treatment.

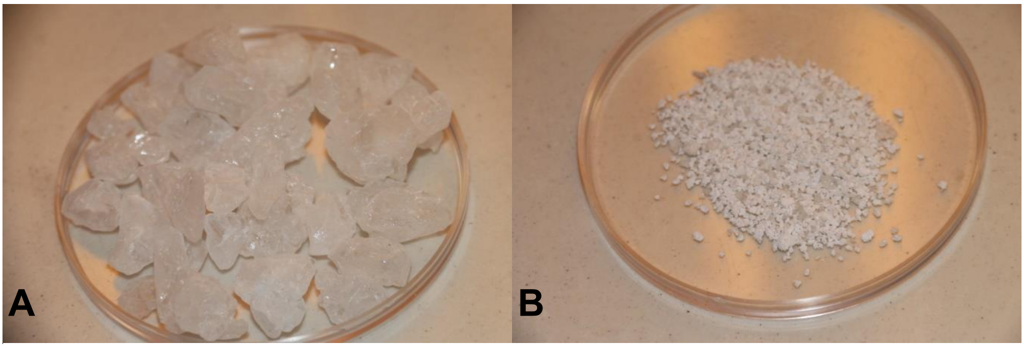

Figure 1. Ammonium aluminium sulphate. A: before thermal treatment and crushing; B: after thermal treatment and crushing.

Characterization of ammonium aluminum sulfate: Determination of adsorbent surface morphology was done by using scanning electron microscopy (Vega\Tescan-Lmu).

Adsorption experiments: Ammonium aluminum sulfate was treated at various temperatures including 200, 300, 350, and 400ºC and for a time of 30 min in order to find the best temperature for proper activation. At a furnace time of less than 30 min, the solid form of ammonium aluminum sulfate deformed like paraffin which may not have acted as an adsorbent. Therefore, we selected 30 min for the treatment because at exactly 30 min the paraffin form converts into a solid form. A comparison between ammonium aluminum sulfate and thermally treated ammonium aluminum sulfate for the removal of fluoride from aqueous solution is shown graphically in Figure 2. As can be seen in the figure, the highest removal percentage of fluoride was observed for the adsorbent prepared at 350ºC.

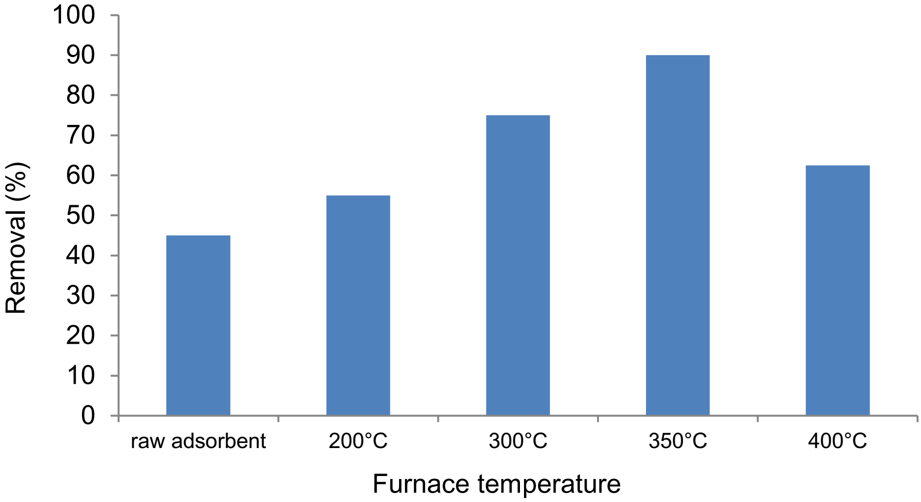

Figure 2. Comparison between ammonium aluminum sulfate and thermally treated ammonium aluminum sulfate for the removal of fluoride.

In this study, the influence of the independent variables such as the initial concentrations of fluoride, the sorbent dosage, the contact time and the pH on the removal efficiency of fluoride was investigated. In the beginning, a stock solution of fluoride with a concentration 1000 ppm in 1 L of deionized water was prepared. The pH of the solutions containing the desired concentrations of fluoride was adjusted by using 0.1N HCl and NaOH. Different doses of adsorbent were added to 50 mL of the fluoride solutions and were shaken for a predetermined time. After shaking, the solutions were filtered using a 0.45 µm membrane filter and the residual concentration of fluoride was analyzed by a UV-visible spectrophotometer. All the batch adsorption experiments were conducted at temperature 25ºC and 150 rpm. All experiments were carried out in duplicate and the results were reported as mean values. Fluoride removal efficiency was calculated from Equation (1):

$$\text{Removal (\%)} = \frac{C_0 - C_e}{C_0} \times 100 \qquad (1)$$

Where:

C_0 is the initial concentration of fluoride (mg/L)
C_e is the equilibrium concentration of fluoride (mg/L)

Experimental design and data analysis: Response surface methodology (RSM), based on central composite design (CCD), was applied to investigate the effect of the independent variables such as the initial concentration of fluoride (A), the adsorbent dosage (B), the contact time (C), and the pH (D) on fluoride adsorption from synthetic aqueous solutions by AAS. Also, this method can predict the main and the interactional effects between the different factors and the optimizing of the adsorption process to achieve the desired objective. In this study, the levels of the independent variables were coded as ±1 (factorial points), ±2 (axial points), and 0 (center point) as shown in Table 1. Also, the alpha value chosen was 2 ($\alpha = 2$). The data range was selected based on studies in the literature and preliminary experiments.[32,33] The independent variables in these experiments were coded based on the following equation:

$$A_i = \frac{X_i - X_0}{\Delta X} \qquad (2)$$

Where:

A_i is the dimensionless coded value of the independent variable
X_i is the uncoded value of the independent variable
X_0 is the value of uncoded independent variable at the center point
ΔX is the step change

The number of 38 runs was designed so that the runs carried out were: 16 runs at factorial points, 16 runs at axial points, and 6 replicates at the center point for the evaluation of the pure error. This process was analyzed by a model of the linear polynomial, the simplest polynomial model, that is shown in following equation.

$$Y = \beta_0 + \sum \beta_i x_i \qquad (3)$$

Where:

Y is the removal efficiency of fluoride
β_0 is a constant amount
β_i is the regression coefficient for linear effects
x_i is the independent variable

The results were analyzed using Design-Expert®, version 7.0.0, statistical software and interpreted by the analysis of variance (ANOVA). The F value and the p value were applied to determine the significance of the models. The adequacy of the model was confirmed by a lack of fit test (any of many tests of a null hypothesis that a proposed statistical model fits well).[1,34]

Table 1. Experimental range and levels of the independent variables (fluoride concentration [A], adsorbent dosage [B], contact time [C], and pH [D])

Independent variable	Unit	Coded level				
		–2	–1	0	1	2
Fluoride concentration (A)	mg/L	2	6.5	11	15.5	20
Adsorbent dosage (B)	g/L	1	3.25	5.5	7.75	10
Contact time (C)	min	2	16.5	31	45.5	60
pH (D)	–	2	4.5	7	9.5	12

RESULTS AND DISCUSSION

Adsorbent characterization: Figure 3 shows the SEM image of the alum nanoparticles. According to the results of the SEM image, the range of the size of the alum nanoparticles is 21–33 nm and the average of nanoparticle size is about 26 nm. As the figure shows, the accumulated nanoparticles have spherical morphologies.

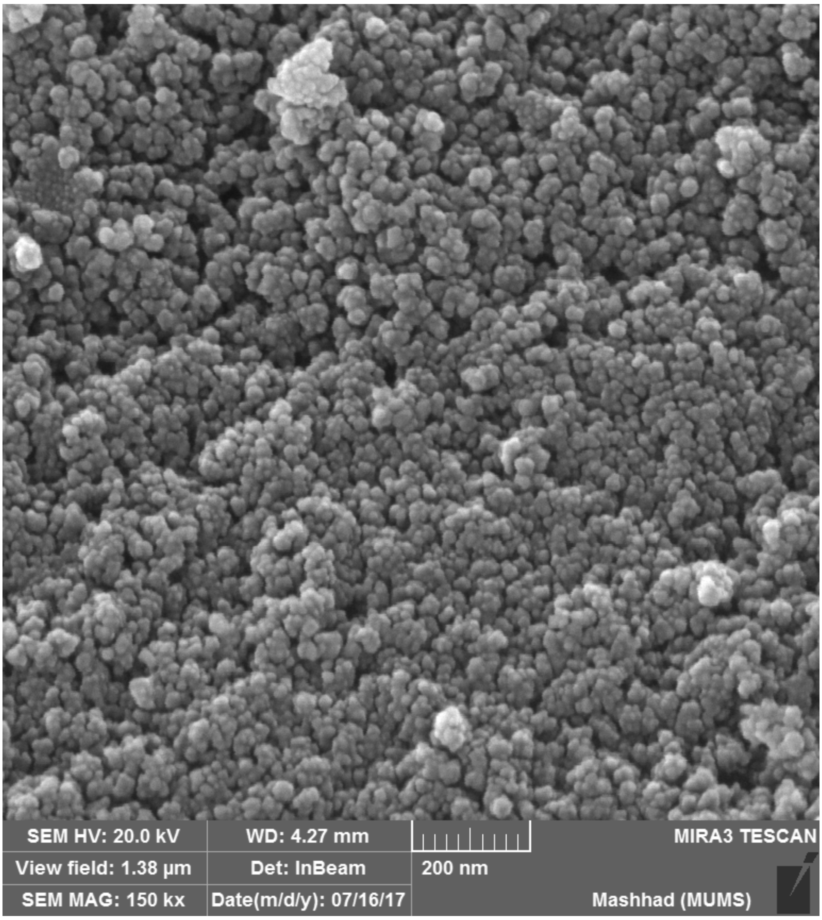

Figure 3. Scanning electron microscopy (SEM) image of the structure of the thermally treated ammonium aluminium sulfate (AAS).

Also, electron-stimulated desorption (EDS) analysis was performed to investigate the chemical composition of the alum nanoparticles. In the EDS spectrum of the AAS, the peaks of the elements of Al, S, and O were observed (Figure 4).

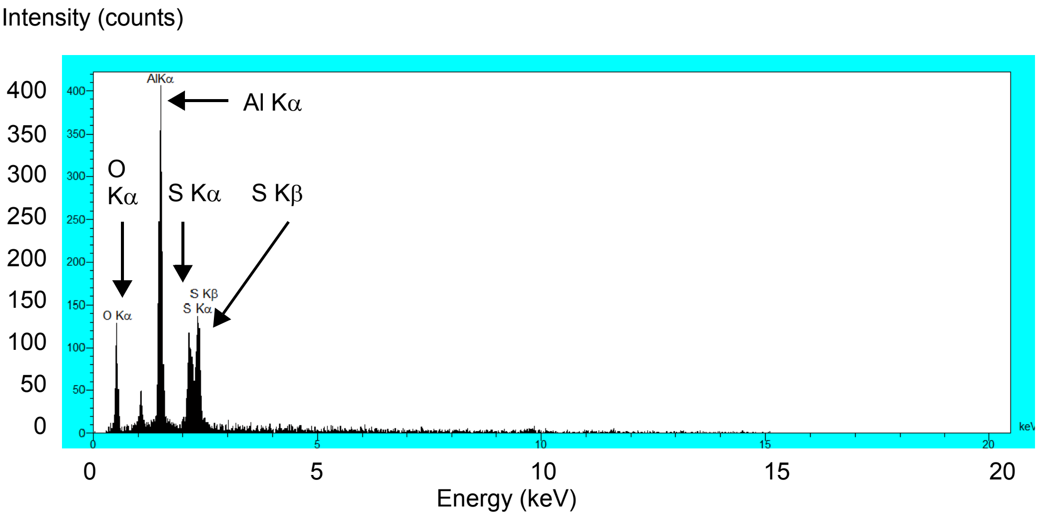

Figure 4. The electron-stimulated desorption (EDS) spectrum of ammonium aluminium sulfate (AAS).

Evaluation of experimental results using RSM: The results of the experiments according to the central composite design are shown in Tables 2A and 2B.

Table 2A. Response values based on central composite design (CCD) for runs 1 to 27

Run order	Fluoride concentration (ppm)	pH	Adsorbent dose (g/L)	Contact time (min)	F removal (%)
1	11.00	2.00	5.50	31.00	53
2	20.00	7.00	5.50	31.00	79
3	15.50	9.50	3.25	45.50	97
4	11.00	12.00	5.50	31.00	100
5	6.50	9.50	7.75	16.50	95
6	11.00	7.00	1.00	31.00	91
7	11.00	7.00	5.50	60.00	69
8	15.50	4.50	7.75	16.50	55
9	6.50	4.50	3.25	45.50	68
10	6.50	4.50	7.75	16.50	59
11	15.50	4.50	3.25	45.50	70
12	6.50	9.50	3.25	45.50	100
13	11.00	7.00	5.50	31.00	78
14	6.50	9.50	3.25	16.50	100
15	2.00	7.00	5.50	31.00	81
16	11.00	7.00	5.50	31.00	79
17	6.50	9.50	7.75	45.50	82
18	15.50	9.50	7.75	45.50	80
19	11.00	7.00	10.00	31.00	60
20	11.00	7.00	5.50	60.00	70
21	11.00	7.00	5.50	31.00	78
22	15.50	9.50	7.75	16.50	85
23	11.00	2.00	5.50	31.00	45
24	20.00	7.00	5.50	31.00	73
25	11.00	7.00	5.50	31.00	77
26	2.00	7.00	5.50	31.00	80
27	15.50	4.50	7.75	45.50	53

Table 2B. Response values based on central composite design (CCD) for runs 28 to 38

Run order	Fluoride concentration (ppm)	pH	Adsorbent dose (g/L)	Contact time (min)	F removal (%)
28	11.00	7.00	5.50	2.00	86
29	15.50	4.50	3.25	16.50	74
30	6.50	4.50	7.75	45.50	57
31	11.00	7.00	10.00	31.00	60
32	11.00	12.00	5.50	31.00	100
33	11.00	7.00	1.00	31.00	94
34	11.00	7.00	5.50	2.00	84
35	11.00	7.00	5.50	31.00	79
36	15.50	9.50	3.25	16.50	97
37	6.50	4.50	3.25	16.50	76
38	11.00	7.00	5.50	31.00	78

The adequacy and the significance of the developed model were determined by the analysis of variance (ANOVA). The analysis of variance and the results obtained from the regression analysis are presented in Table 3.

Table 3. ANOVA of the response surface linear model for fluoride removal (df=degrees of freedom)

Source	Sum of squares	df	Mean square	F value	p value
Model	7964.13	4	1991.03	259.56	<0.0001
A-Fluoride concentration	60.5	1	60.5	7.89	0.0083
B-Adsorbent dose	1891.13	1	1891.13	246.53	< 0.0001
C-Time	288	1	288	37.54	< 0.0001
D-pH	5724.5	1	5724.5	746.27	< 0.0001
Residual	253.14	33	7.67		
Lack of fit	192.8	20	9.64	2.08	0.0895
Pure error	60.33	13	4.64		
Correlation total	8217.26	37			

Note: R-squared: 0.97; adjusted R-squared: 0.9655; predicted R-squared: 0.9575 (The adjusted R-squared is used to compare the goodness-of-fit for regression models that contain differing numbers of independent variables. The predicted R-squared is used to determine how well a regression model makes predictions.)

As shown in Table 3, the F and p values for the linear model are 259.56 and less than 0.0001, respectively. The large F value and the small p value point to a high level of statistical significance for the model. The p values less than 0.05 for the model terms (A, B, C, and D) demonstrate that these are significant.[35] The R^2, adjusted R^2, and predicted R^2 values were 0.97, 0.96, and 0.95, respectively, which indicates that there is a good correlation between the predicted and the actual values. Also the high R^2 value indicates that the model is statistically valid. The corresponding value for the lack of fit was 0.0895 (statistically insignificant) which suggests a good fitted model.[31,36] The coefficient of variation (CV) implies the ratio of the standard error to the mean value of the observed response. In this model, the CV value of 3.58 indicates that the model was favorable.

The coded linear equation was given by Design-Expert®software in which the empirical relationship between the independent variables and the removal efficiency of fluoride (%) was described. This equation (4) in terms of the coded factors is shown as:

$$\text{Fluoride removal} = (77.42) - (1.38\,A) - (7.69\,B) - (3.00\,C) + (13.38\,D) \quad (4)$$

Where:

A = initial fluoride concentration (mg/L)
B = sorbent dosage (g/L)
C = contact time (min)
D = solution pH

In equation (4), the negative coefficients for the model parameters A, B, and C indicate that these parameters had an antagonistic effect on fluoride removal and the positive coefficient for the model parameters D shows that this parameter had the effect of enhancing fluoride removal.

A plot of the predicted results versus the experimental results for fluoride removal is shown in Figure 5. As can be observed, there is good agreement between the experimental values and the predicted values for fluoride removal by AAS.

Effect of initial fluoride concentration and adsorbent dose: Figure 6 depicts the effect of the initial fluoride concentration on the fluoride removal percentage by AAS at an adsorbent dose of 5.50 g/L, a time of 31 min, and a pH of 7. As shown, an increase in the initial concentration of fluoride results in a decrease of the removal efficiency of fluoride due to the lower availability of binding sites for the adsorption of fluoride onto the AAS surface. As seen in Figure 7, increasing the sorbent dosage from 3.25 to 7.75 causes a decrease in the fluoride removal from 85% to 70%. Overall, a lower sorbent dosage and a lower fluoride concentration increased the removal percentage.

Effect of pH: The effect of pH on the removal percentage of fluoride is presented in Figure 8. It is obvious that the removal efficiency of fluoride increased when the pH of the solution increased from 4.5 to 9.5. In the acidic pH range, the removal percentage of fluoride deceased which may be due to an electrostatic and chemical interaction between the adsorbent surface and the fluoride ion or the formation of weak hydrofluoric acid.[37] In an alkaline pH range with a pH > 7, the adsorption of fluoride is very high compared to that with an acidic pH. The maximum removal of fluoride occurred at pH 9.5.

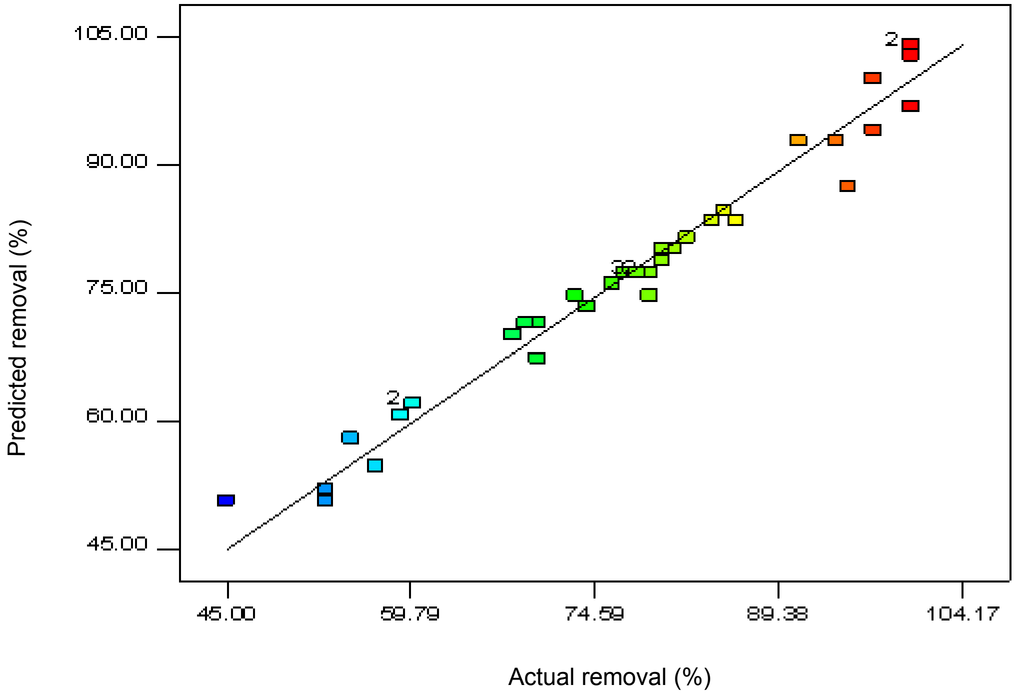

Figure 5. Predicted vs. actual values of the removal efficiency of fluoride.

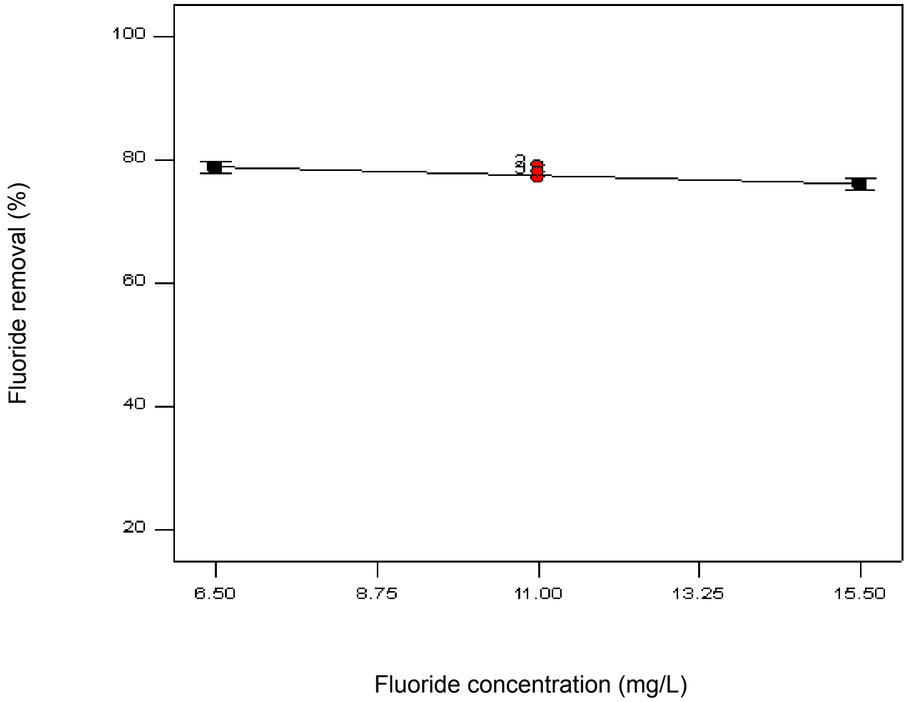

Figure 6. Effect of fluoride concentration on the removal percentage of fluoride by ammonium aluminium sulphate (AAS).

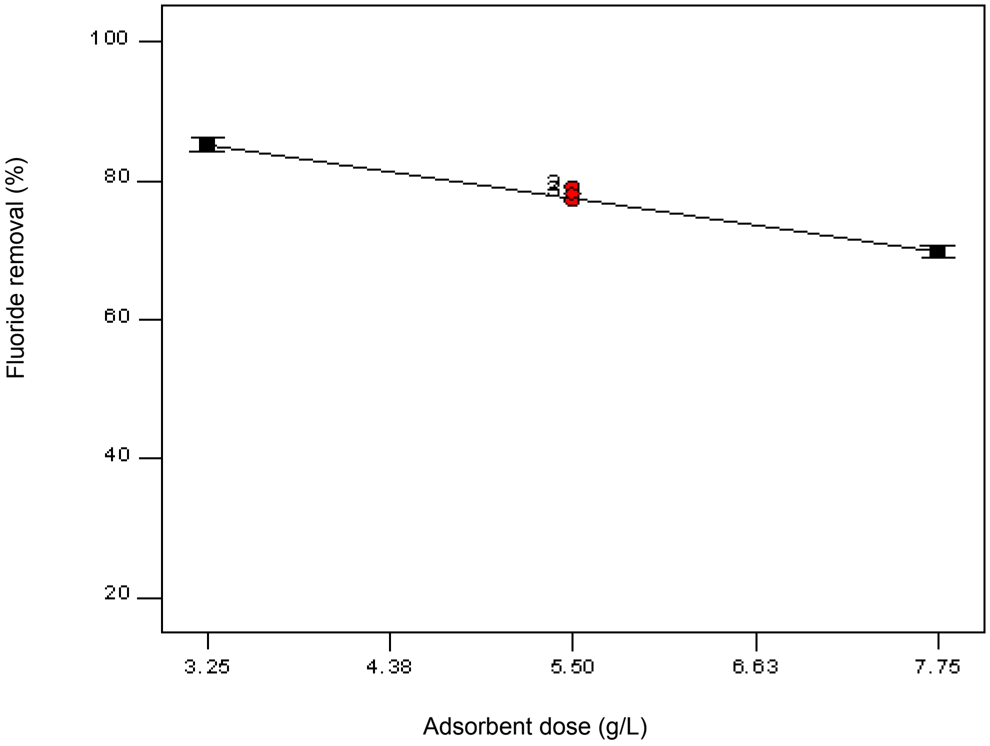

Figure 7. Effect of adsorbent dose on the removal percentage of fluoride by ammonium aluminium sulphate (AAS).

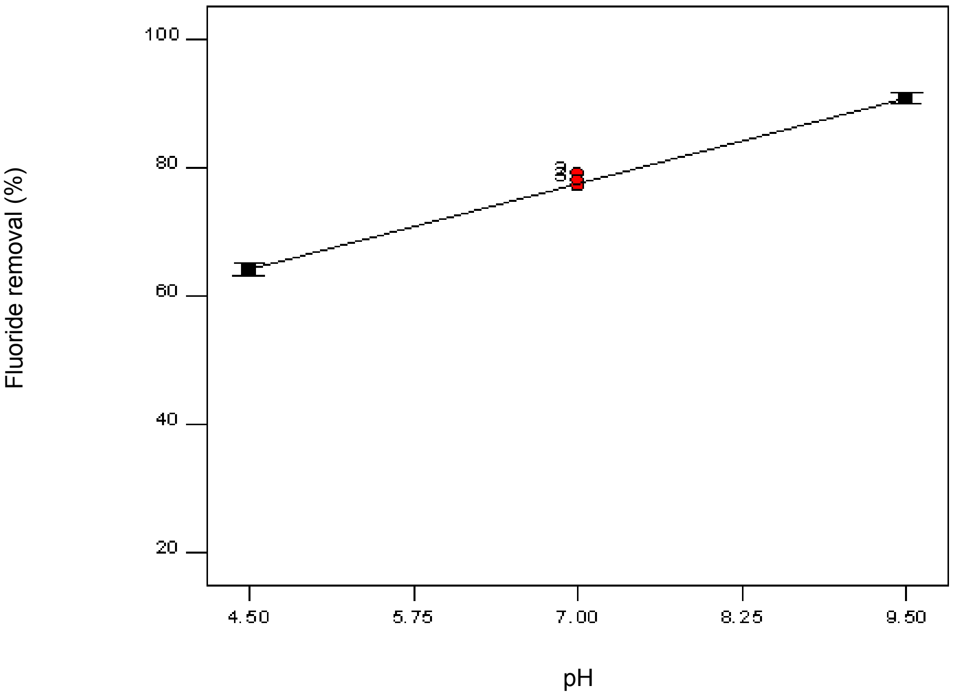

Figure 8. Effect of pH on the removal percentage of fluoride by ammonium aluminium sulphate (AAS).

Effect of contact time: The removal of fluoride ions declined as the contact time increased (Figure 9). The fluoride uptake was rapid during the initial contact time. This means that only a short time is needed for the fluoride ions to make an attractive complex with the AAS.

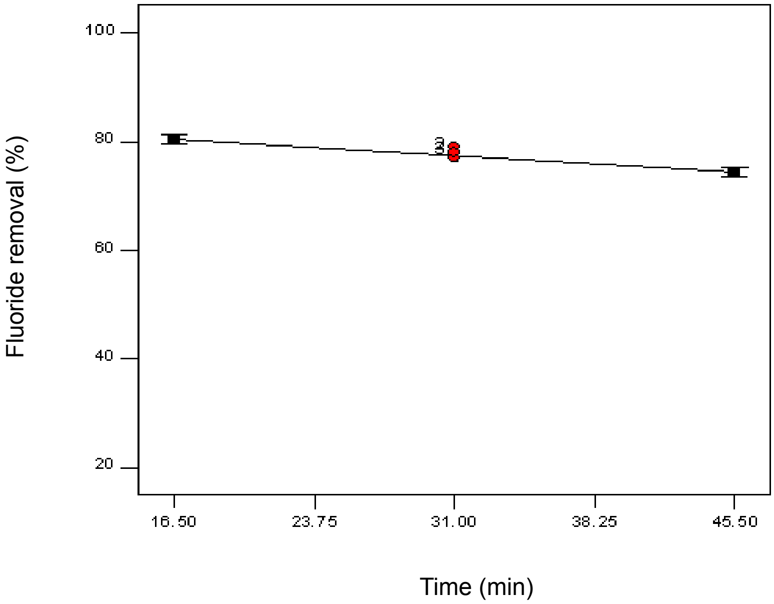

Figure 9. Effect of time on the removal percentage of fluoride by ammonium aluminium sulphate (AAS).

Process optimization and confirmation: The optimum conditions for fluoride removal were determined. The predicted optimum values were: an initial fluoride concentration of 6.80 mg/L, a sorbent dosage of 3.25 g/L, a pH of 9, and a contact time of 16.50 min. To investigate the validity of the predicted results, several additional experiments were conducted and the results indicated that there was a good correlation between the experimental responses and the predicted one (Figure 5).

Kinetics of fluoride adsorption: In order to describe the kinetic parameters of fluoride adsorption on AAS, two models, the pseudo first-order and the pseudo second order, were used. The pseudo first-order form can be represented using the following equation:

$$\log(q_e - q_t) = \log(q_e) - \frac{k_1}{2.203} t \qquad (5)$$

Where:

q_e is the absorption capacity for fluoride of ammonium aluminium sulfate (mg/g) at equilibrium

q_t is the absorption capacity for fluoride of ammonium aluminium sulfate (mg/g) at time t

k_1 (min^{-1}) is the rate constant of adsorption which can be calculated from the slope of the linear plot of log ($q_e - q_t$) versus time

q_e and q_t are the adsorption capacity for fluoride of ammonium aluminium sulfate (mg/g) at equilibrium and time t, respectively. k_1 (min^{-1}) is the rate constant of adsorption which can be calculated from the slope of the linear plot of log (q_e – q_t) versus time.

The pseudo second-order equation was defined as:

$$\frac{t}{q_t} = \frac{1}{k_2\, q_e^{\,2}} + \frac{t}{q_e} \qquad (6)$$

Where:

k_2 is the rate constant for the pseudo second order adsorption (min-1). It is given by the slope of the plot of t/q_t versus t [37]

q_e is given by the intercept of the plot of t/q_t versus t [37]

The intraparticle diffusion model was explored by using following equations:

$$Q_t = K_p\,(t^{0.5}) + C \qquad (7)$$

Where:

Kp is the intra-particle diffusion constant and was obtained by the slope of the plot of Q_t against $t^{0.5}$

C is the intra-particle diffusion intercept

In this equation, information related to the thickness of the boundary layer was determined by C. The values of K_p and C are the intra-particle diffusion constant and intercept, respectively. K_p was obtained from the slope of the plot of q_t against $t^{0.5}$.

The kinetic parameters and the correlation coefficient for fluoride adsorption by AAS are represented in Table 4. The results of the adsorption kinetics revealed that the pseudo-second order model with the correlations coefficient of $R^2 = 0.99$ gave the best fit.

Table 4. Kinetic parameters and correlation coefficient for fluoride adsorption by AAS
C=concentrataion of fluoride (mg/L)

C	Pseudo first order				Pseudo second order			Intraparticle diffusion	
(mg/L)	q_e, exp. (mg/g)	q_e (mg/g)	K_1 (min^{-1})	R^2	q_e (mg/g)	K_1 (min^{-1})	R^2	K_2 (mg/g min$^{-0.5}$)	R^2
5	2	0.46	0.006	0.81	1.31	0.653	0.99	0.047	0.90
10	4.5	1.41	0.003	0.82	2.75	0.404	0.99	0.048	0.72
15	6.2	1.65	0.005	0.90	4.13	0.403	0.99	0.073	0.88

The fitting of the experimental data with the pseudo-first-order, the pseudo-second-order, and the intraparticle diffusion kinetic models is shown in Figure 10.

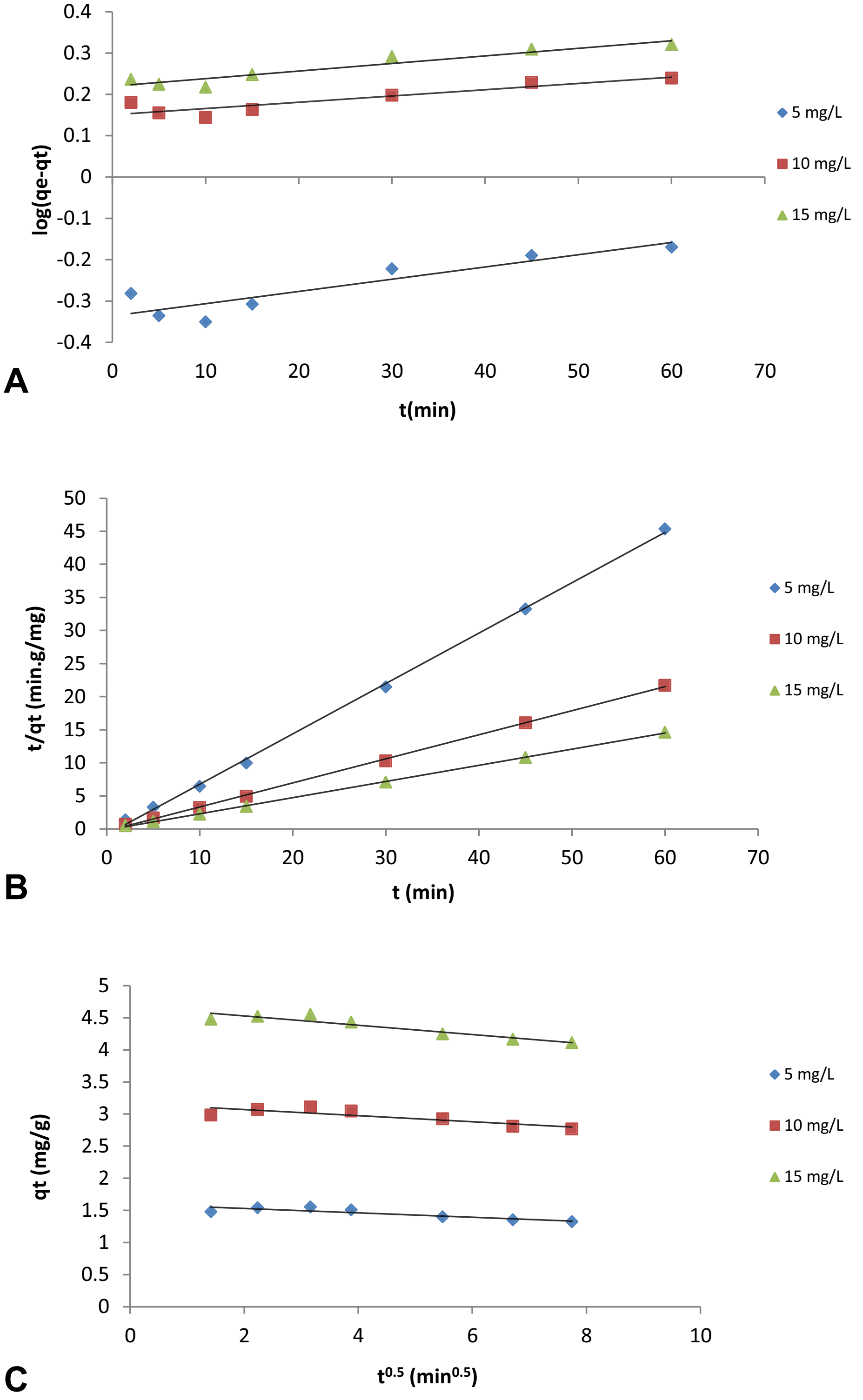

Figure 10. Fitting the experimental data to the kinetic models. A: the pseudo-first-order kinetic model; B: the pseudo-second-order kinetic model; and C: the intraparticle diffusion kinetic model.

Adsorption isotherms studies: Isothermal studies were performed to evaluate the adsorption mechanism of fluoride on to the AAS. From among several isotherm models, four isotherm models was selected, i.e., Langmuir, Freundlich, Temkin, and Dubinin–Radushkevich (D–R). The Langmuir isotherm describes monolayer adsorption which in its linearized form can be expressed by following equation:

$$\frac{C_e}{q_e} = \frac{1}{K_L q_{max}} + \frac{1}{q_{max}} C_e \qquad (8)$$

The Freundlich isotherm indicates the multilayer adsorption of contaminants on to an adsorbent surface and the linear form of this isotherm is given by:

$$\ln q_e = \ln K_F + \frac{1}{n} \ln C_e \qquad (9)$$

The Temkin and Dubinin–Radushkevich (D–R) isotherm models were also represented by following equations, respectively:

$$q_e = B \ln A + B \ln C_e \qquad (10)$$

$$\ln q_e = \ln q_m - K\, \varepsilon^2 \qquad (11)$$

In these equations, C_e and q_e are the equilibrium concentration of fluoride (mg/L) and adsorption capacity at equilibrium (mg/g), q_m is the maximum adsorption capacity for the Langmuir isotherm (mg/g), K_L is the Langmuir adsorption constant (L/mg), K_F and n are the Freundlich constants that expresses adsorption capacity and adsorption intensity, respectively, and can be calculated from the slope and intercept of the plot of $\ln(q_e)$ versus $\ln(C_e)$. B is a constant corresponding to the heat of adsorption and A is the Temkin binding constant (L/g). B is the Polanyi potential which can be calculated by RT ln(1+1/Ce), where R and T are the gas constant and temperature (Kelvin), respectively. Also, K is the adsorption energy constant.[25,39]

The adsorption isotherm studies were conducted under optimized conditions (pH = 9, adsorbent dosage = 3.25 g/L, and temperature = 25ºC), fluoride concentrations ranging from 5 to 50 mg/L and a contact time of 60 min (Figures 11A–11D). As presented in Table 5, the maximum adsorption capacity of AAS for fluoride was 13.33 mg/g. The comparison of the maximum adsorption capacities of fluoride by the various adsorbents is shown in Table 6. The fluoride adsorption on AAS was well fitted by the Freundlich model with a regression coefficient (R^2) of 0.99. This finding has also been reported in the literature for fluoride removal by other adsorbents.[40,41] Other parameters related to the adsorption isotherms are also summarized in Table 5.

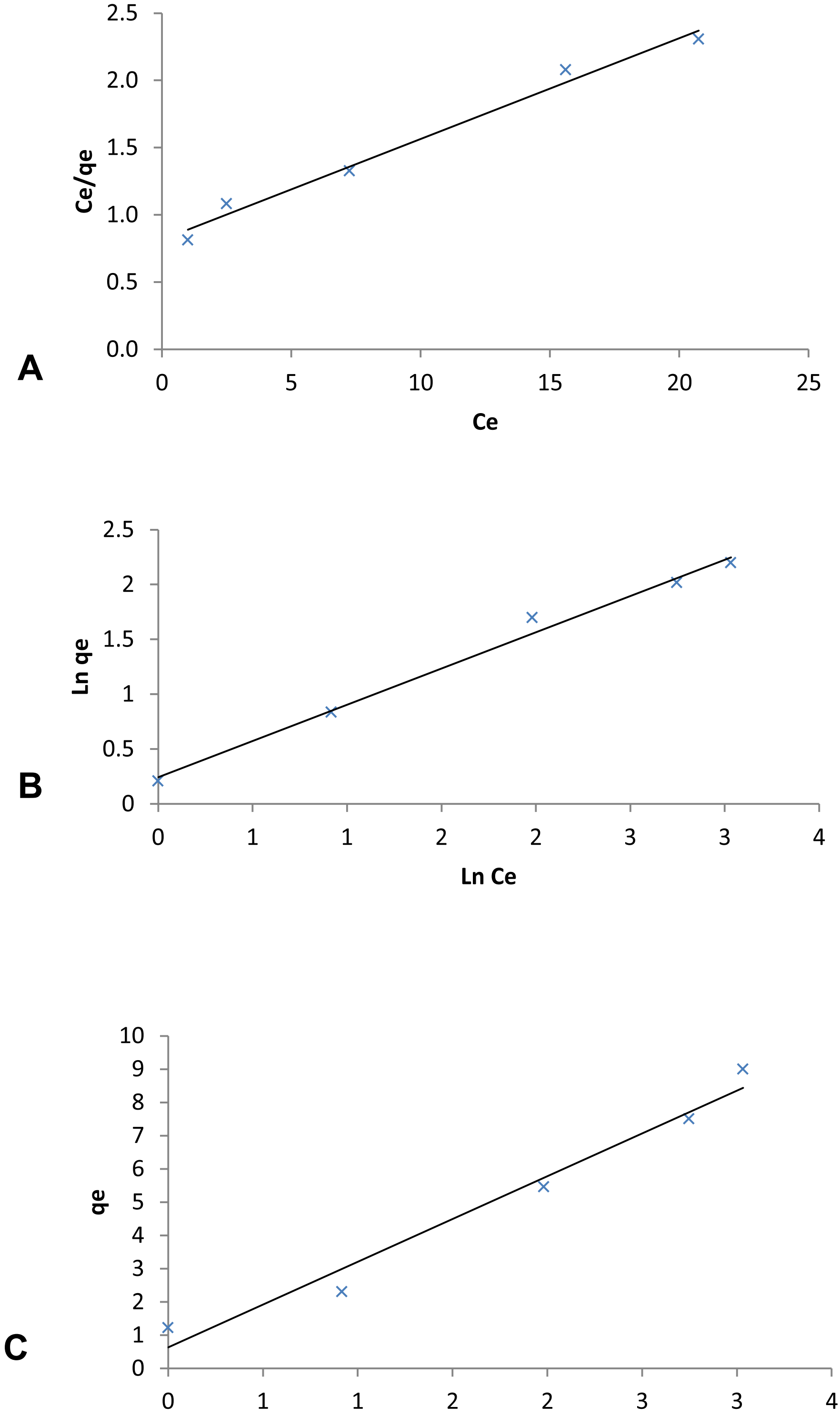

Figures 11A–11C. Plots for the adsorption of fluoride by ammonium aluminium sulphate (AAS) with various isotherm models. A: the Langmuir isotherm model; B: the Freundlich isotherm model; and C: the Temkin isotherm model.

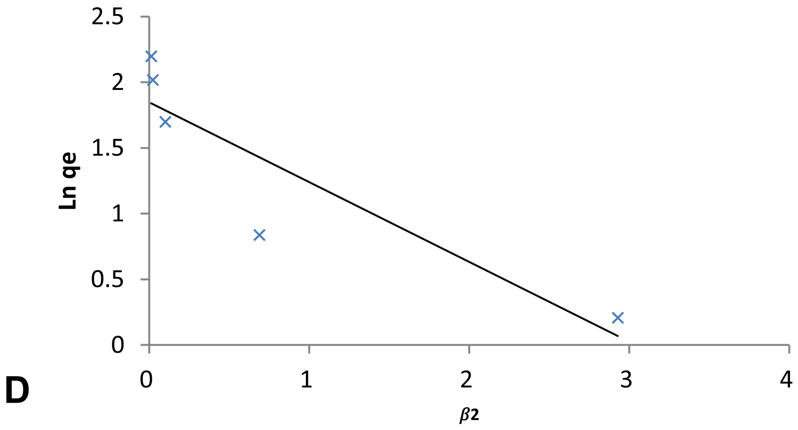

Figure 11D. Plots for the adsorption of fluoride by ammonium aluminium sulphate (AAS) with various isotherm models. D: the Dubinin–Radushkevich (D–R) isotherm model.

Table 5. Isotherm parameters obtained for fluoride adsorption on to ammonium aluminium sulfate (AAS)

Isotherm model	Parameter	Value
Laingmuir	Qmax	13.33
	K_L	0.092
	R^2	0.98
	n	1.51
Freundlich	K_F (mg/g)$([\frac{L}{mmol})]^{\frac{1}{n}}$	1.75
	R^2	0.99
	A	0.92
Temkin	B	2.57
	R^2	0.97
	K	6.07
Dubinin–Radushkevich	q_{max}	6.35
	R^2	0.81

Effect of the temperature on fluoride adsorption: In this study, the effect of temperature on fluoride adsorption, under the optimum conditions of pH = 9, adsorbent dose = 3.25 g/L and a time range of 15–60 min, was evaluated. As shown in Figure 12, a temperature increase from 30 to 50ºC decreased the fluoride removal efficiency during various time periods.

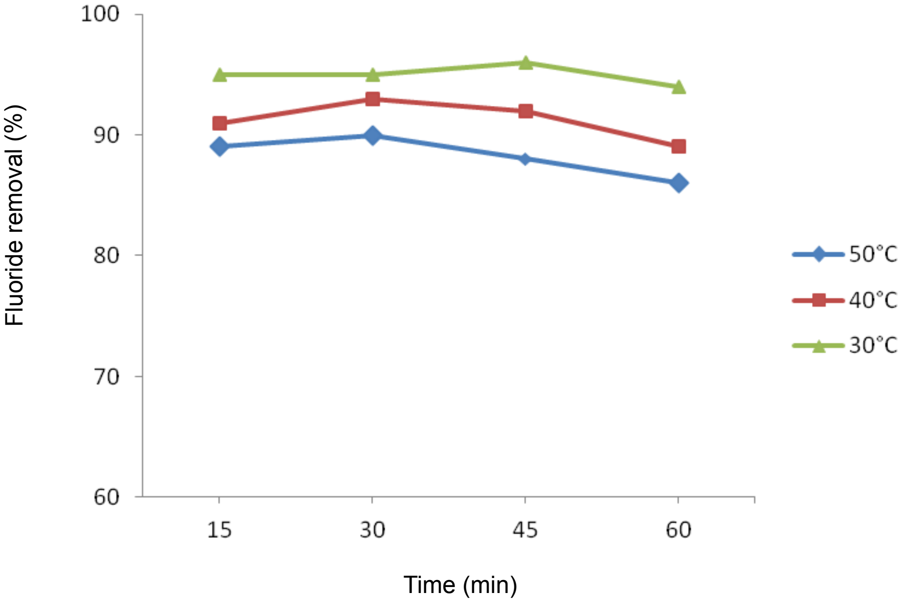

Figure 12. Plot of the effect of temperature on fluoride adsorption by ammonium aluminium sulphate (AAS).

Effect of co-existing anions: Various ions may be present in water and these can affect the removal efficiency of the fluoride from an aquatic solution. In this work, the effect of the interfering ions (chloride, sulfate, nitrate, phosphate, carbonate, and bicarbonate) at different initial concentrations under optimized conditions was assessed. The effect of coexisting ions on fluoride adsorption is shown in Figure 13. Based on the figure, SO_4^{2-} and PO_4^{3-} anions have the highest effect on fluoride removal. The extent of the inhibition of fluoride adsorption by the co-existing anions may be due to the ionic radii. Also, the surface charge densities of PO_4^{3-} and SO_4^{2-} are higher than that of fluoride resulting in competition between the fluoride ion and the other co-existing anions.[46]

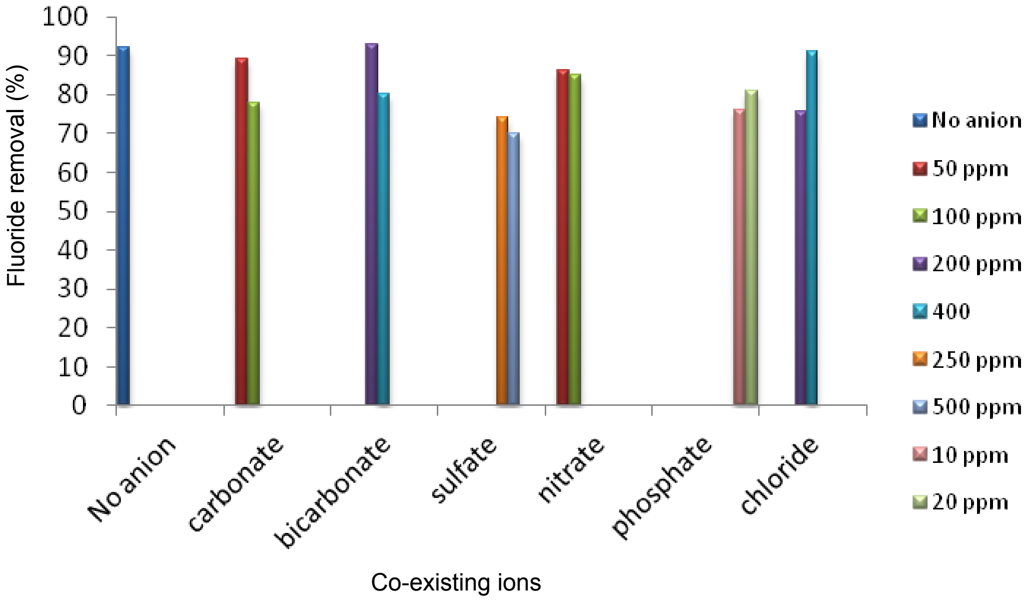

Figure 13. The effect of coexisting ions on fluoride adsorption by ammonium aluminium sulphate (AAS). (Fluoride concentration: 6.80 mg/L; pH: 9; contact time: 16.5 min; AAS: 3.25 g/L).

CONCLUSIONS

The present study indicates that ammonium aluminum sulfate $(NH_4)Al(SO_4)_2$ can be used as an effective adsorbent for the adsorption of fluoride from aqueous solutions. The experiments' design, the data analysis, and the optimization of the adsorption process were performed using RSM. The results illustrated that the best model for predicting fluoride removal is a linear one. The R^2 value of 0.97 implies that there was a good match between the experimental values and the predicted values. The significance of the model was determined by the F value and the p value. The optimum conditions for maximum fluoride adsorption (100%) were determined to be: an initial fluoride concentration of 6.80 mg/L, a sorbent dosage of 3.25 g/L, a pH of 9, and a contact time of 16.50 min. Of four isotherm models studied, the results obtained fitted well (R^2=0.99) with both the Freundlich model, which showed a maximum adsorption capacity of 13.33 mg/g, and the pseudo-second-order kinetic model. The presence of co-existing anions decreased fluoride adsorption in the following order: $SO_4^{2-} > PO_4^{3-} > NO_3^{-} > Cl^{-} > CO_3^{2-} > HCO_3^{-}$.

ACKNOWLEDGEMENTS

The authors thank the Gonabad University of Medical Sciences for financial support.

REFERENCES

1 Rehman MA, Yusoff I, Alias Y. Fluoride adsorption by doped and un-doped magnetic ferrites CuCexFe 2-x O 4: Preparation, characterization, optimization and modeling for effectual remediation technologies. Journal of Hazardous Materials 2015;299:316-24.

2 Yousefi M, Ghoochani M, Mahvi AH. Health risk assessment to fluoride in drinking water of rural residents living in the Poldasht city, Northwest of Iran. Ecotoxicol Environ Saf 2018; 148:426-30.

3 Dobaradaran S, Mahvi AH, Dehdashti S, Abadi DRV, Tehran I. Drinking water fluoride and child dental caries in Dashtestan, Iran. Fluoride. 2008;41(3):220-6.

4 Karimzade S, Aghaei M, Mahvi A. Investigation of intelligence quotient in 9–12-year-old children exposed to high-and low-drinking water fluoride in West Azerbaijan Province, Iran. Fluoride 2014;47(1):9-14.

5 Aghaei M, Derakhshani R, Raoof M, Dehghani M, Mahvi AH. Effect of fluoride in drinking water on birth height and weight: an ecological study in Kerman Province, Zarand County, Iran. Fluoride 2015;48(2):160-8.

6 Dobaradaran S, Mahvi AH, Dehdashti S. Fluoride content of bottled drinking water available in Iran. Fluoride 2008;41(1):93-4.

7 Mahvi AH, Ghanbarian M, Ghanbarian M, Khosravi A, Ghanbarian M. Determination of fluoride concentration in powdered milk in Iran 2010. British Journal of Nutrition 2012;107(7):1077-9.

8 Srivastav AL, Singh PK, Srivastava V, Sharma YC. Application of a new adsorbent for fluoride removal from aqueous solutions. Journal of Hazardous Materials 2013;263:342-52.

9 Su C, Wang Y, Xie X, Li J. Aqueous geochemistry of high-fluoride groundwater in Datong Basin, Northern China. Journal of Geochemical Exploration 2013;135:79-92.

10 Nouri J, Mahvi AH, Babaei A, Ahmadpour E. Regional pattern distribution of groundwater fluoride in the Shush aquifer of Khuzestan County, Iran. Fluoride 2006;39(4):321-5.

11 KheradPisheh Z, Ehrampoush MH, Montazeri A, Mirzaei M, Mokhtari M, Mahvi AH. Fluoride in Drinking Water in 31 Provinces of Iran. Journal of Exposure and Health 2016;8(4): 465-74.

12 Rahmani A, Rahmani K, Dobaradaran S, Mahvi AH, Mohamadjani R, Rahmani, H. Child dental caries in relation to fluoride and some inorganic constituents in drinking water in Arsanjan, Iran. Fluoride 2010;43(3):179-86.

13 Aghaei M, Karimzade S, Yaseri M, Khorsandi H, Zolfi E, Mahvi AH. Hypertension and fluoride in drinking water: Case study from West Azerbaijan, Iran. Fluoride 2015;48(3):252-8.

14 Ponsot I, Falcone R, Bernardo E. Stabilization of fluorine-containing industrial waste by production of sintered glass-ceramics. Ceramics International 2013;39(6):6907-15.

15 Dobaradaran S, Fazelinia F, Mahvi AH, Hosseini S S. Particulate airborne fluoride from an aluminium production plant in Arak, Iran. Fluoride 2009;42(3):228-32.

16Mourad N, Sharshar T, Elnimr T, Mousa M. Radioactivity and fluoride contamination derived from a phosphate fertilizer plant in Egypt. Applied Radiation and Isotopes 2009;67(7):1259-68.

17 Warmadewanthi B, Liu J. Selective separation of phosphate and fluoride from semiconductor wastewater. Water Science and Technology 2009;59(10):2047-53.

18 Boldaji MR, Mahvi A, Dobaradaran S, Hosseini S. Evaluating the effectiveness of a hybrid sorbent resin in removing fluoride from water. International Journal of Environmental Science & Technology 2009;6(4):629-32.

19 Zhang S, Lu Y, Lin X, Su X, Zhang Y. Removal of fluoride from groundwater by adsorption onto La (III)-Al (III) loaded scoria adsorbent. Applied Surface Science 2014;303:1-5.

20 Shen J, Schäfer AI. Factors affecting fluoride and natural organic matter (NOM) removal from natural waters in Tanzania by nanofiltration/reverse osmosis. Sci Total Environ 2015;527:520-9.

21 Lahnid S, Tahaikt M, Elaroui K, Idrissi I, Hafsi M, Laaziz I, et al. Economic evaluation of fluoride removal by electrodialysis. Desalination 2008;230(1-3):213-9.

22 Kir E, Alkan E. Fluoride removal by Donnan dialysis with plasma-modified and unmodified anion-exchange membranes. Desalination 2006;197(1-3):217-24.

23 Simons R. Trace element removal from ash dam waters by nanofiltration and diffusion dialysis. Desalination 1993;89(3):325-41.

24 Qiusheng Z, Xiaoyan L, Jin Q, Jing W, Xuegang L. Porous zirconium alginate beads adsorbent for fluoride adsorption from aqueous solutions. RSC Advances 2015;5(3):2100-12.

25 Zazouli MA, Mahvi AH, Dobaradaran S, Barafrashtehpour M, Mahdavi Y, Balarak D. Adsorption of fluoride from aqueous solution by modified *Azolla filiculoides*. Fluoride 2014;47 (4):349-58.

26 Mohapatra M, Anand S, Mishra BK, Giles DE, Singh P. Review of fluoride removal from drinking water. Journal of Environmental Management 2009;91(1):67-77.

27 Davila-Rodriguez JL, Escobar-Barrios VA, Rangel-Mendez JR. Removal of fluoride from drinking water by a chitin-based biocomposite in fixed-bed columns. Journal of Fluorine Chemistry 2012;140:99-103.

28 Gómez-Hortigüela L, Pérez-Pariente J, García R, Chebude Y, Díaz I. Natural zeolites from Ethiopia for elimination of fluoride from drinking water. Separation and Purification Technology 2013;120:224-9.

29 Kang D, Yu X, Tong S, Ge M, Zuo J, Cao C, et al. Performance and mechanism of Mg/Fe layered double hydroxides for fluoride and arsenate removal from aqueous solution. Chemical Engineering Journal 2013;228:731-40.

30Elvers B, Hawkins S, Russey WE. Ullmann’s encyclopedia of industrial chemistry. Wiley Online Library. Weinheim, Germany: Wiley-VCH Verlag GmbH & Co. KGaA.; 2000.

31 Mourabet M, El Rhilassi A, El Boujaady H, Bennani-Ziatni M, El Hamri R, Taitai A. Removal of fluoride from aqueous solution by adsorption on hydroxyapatite (HAp) using response surface methodology. Journal of Saudi Chemical Society 2015;19(6):603-15.

32 Kumar E, Bhatnagar A, Ji M, Jung W, Lee S-H, Kim S-J, et al. Defluoridation from aqueous solutions by granular ferric hydroxide (GFH). Water Research 2009;43(2):490-8.

33 Kang J, Li B, Song J, Li D, Yang J, Zhan W, et al. Defluoridation of water using calcined magnesia/pullulan composite. Chemical Engineering Journal 2011;166(2):765-71.

34 Witek-Krowiak A, Chojnacka K, Podstawczyk D, Dawiec A, Pokomeda K. Application of response surface methodology and artificial neural network methods in modelling and optimization of biosorption process. Bioresource Technology 2014;160:150-60.

35 Fakhri A. Application of response surface methodology to optimize the process variables for fluoride ion removal using maghemite nanoparticles. Journal of Saudi Chemical Society 2014;18(4):340-7.

36 Mourabet M, El Rhilassi A, El Boujaady H, Bennani-Ziatni M, Taitai A. Use of response surface methodology for optimization of fluoride adsorption in an aqueous solution by Brushite. Arabian Journal of Chemistry 2017;10(Suppl 2):S3292-302.

37 Tripathy SS, Bersillon J-L, Gopal K. Removal of fluoride from drinking water by adsorption onto alum-impregnated activated alumina. Separation and Purification Technology 2006;50(3):310-7.

38 Bazrafshan E, Balarak D, Panahi AH, Kamani H, Mahvi AH. Fluoride removal from aqueous solutions by cupricoxide nanoparticles. Fluoride 2016;49(3):233-44.

39 Swain S, Patnaik T, Patnaik P, Jha U, Dey R. Development of new alginate entrapped Fe (III)–Zr (IV) binary mixed oxide for removal of fluoride from water bodies. Chemical Engineering Journal 2013;215:763-71.

40 Viswanathan N, Meenakshi S. Enriched fluoride sorption using alumina/chitosan composite. Journal of Hazardous Materials 2010;178(1):226-32.

41 Dou X, Zhang Y, Wang H, Wang T, Wang Y. Performance of granular zirconium–iron oxide in the removal of fluoride from drinking water. Water Research 2011;45(12):3571-8.

42 Sun Y, Fang Q, Dong J, Cheng X, Xu J. Removal of fluoride from drinking water by natural stilbite zeolite modified with Fe (III). Desalination 2011;277(1):121-7.

43 Ma Y, Shi F, Zheng X, Ma J, Gao C. Removal of fluoride from aqueous solution using granular acid-treated bentonite (GHB): Batch and column studies. Journal of Hazardous Materials 2011;185(2):1073-80.

44 Sujana M, Anand S. Fluoride removal studies from contaminated ground water by using bauxite. Desalination 2011;267(2):222-7.

45 Salifu A, Petrusevski B, Ghebremichael K, Modestus L, Buamah R, Aubry C, et al. Aluminum (hydr) oxide coated pumice for fluoride removal from drinking water: Synthesis, equilibrium, kinetics and mechanism. Chemical Engineering Journal 2013;228:63-74.

46 Kusrini E, Sofyan N, Suwartha N, Yesya G, Priadi CR. Chitosan-praseodymium complex for adsorption of fluoride ions from water. Journal of Rare Earths 2015;33(10):1104-13.